

## STRESSES AROUND TWO EQUAL REINFORCED CIRCULAR OPENINGS IN A THIN PLATE

SURENDRA K. DHIR

Naval Ship Research and Development Center, Washington, D.C. 20007

**Abstract**—An analytical solution is presented for the stresses around two circular openings of equal size in a thin elastic plate of isotropic material under biaxial loads. The openings can be either unreinforced or reinforced. The reinforcing material, which is the same as that of the parent plate, is assumed to be concentrated around the boundaries of the openings. The stresses are obtained in bipolar coordinates as infinite series. Numerical convergence of this series is governed by the ratio of the size and spacing of the two openings. The results are computed on a high speed digital computer as stress concentration factors for a number of hole geometries and reinforcements which frequently occur in practice.

### NOTATION

$A$	area of cross-section of the reinforcing ring
$A_n, B_n, K$	coefficients of auxiliary stress function
$a_n, b_n, c_n, a'_n, b'_n, c'_n$	constants in the equations for determination of $A_n, B_n, K$
$aT, bT$	applied stresses
$d$	distance of poles from origin in bipolar coordinates
$ds, d\theta$	length and angular increment
$F$	stress function in bipolar coordinates
$F_0, F_a$	fundamental and auxiliary stress functions respectively
$h_{1,n}, h_{2,n}, h_{3,n}$	coefficients of stresses in series form
$n$	running index
$P, R, S$	circumferential, radial, shear forces respectively in reinforcing ring
$t$	thickness of plate
$x, y$	Cartesian coordinates
$z$	$x + iy$
$\xi, \eta$	bipolar coordinates
$\zeta$	$\xi + i\eta$
$\theta$	polar angle
$\alpha'$	$A/t$
$\widehat{\xi\xi}, \widehat{\eta\eta}, \widehat{\xi\eta}$	stress components in bipolar coordinates
$\sigma_E$	equivalent stress from maximum strain energy of distortion $(\sigma_E = [\widehat{\xi\xi}^2 + \widehat{\eta\eta}^2 - \widehat{\xi\xi}\widehat{\eta\eta} + 3\widehat{\xi\eta}^2]^{1/2})$

### INTRODUCTION

THE general stress solution for plane problems involving two nonconcentric circular boundaries was first obtained by Jeffery [1]. This solution in bipolar coordinates had applications to manifold problems, viz. a cylinder or pipe with eccentric bore [1], a semi-infinite plate with a circular hole near the edge [1, 2], and a large plate containing two circular openings [1, 3]. The solutions involving both a finite and an infinite boundary were, however, limited to simpler boundary conditions, i.e., one of the boundaries was load-free. In particular, the problem of two equal circular holes in a large plate was considered in detail by Ling [3], the two circular holes constituted the finite load-free boundary.

In engineering structures, however, these openings are seldom free boundaries since they have to be reinforced.

This paper determines the stresses around two equal circular openings in a large plate under biaxial normal stresses when both the holes are reinforced. The solution which follows is based on the following assumptions:

1. The plate is thin in comparison to the other dimensions and stretches to infinity in both  $x$  and  $y$ -directions.
2. The plate material is elastic, isotropic, and homogeneous.
3. The reinforcing material is the same as that of the parent plate and is thinly distributed around the openings.
4. The reinforcement can be subject to hoop stresses only and has no bending stiffness.

The first two are the usual assumptions for a generalized plane stress system within the theory of elasticity. The third assumption is clearly justified since the openings to be reinforced are usually large compared to the reinforcement. The last assumption is based on the findings of [4] and [5], which suggested that in the case of a single circular reinforced opening, the effect of bending stiffness on the overall stress field is of second order.

The method of solution will be to superimpose on the fundamental state of stress without the openings an auxiliary system of stresses which will not affect the applied loads but will help satisfy the boundary conditions at the reinforced openings. The form of the auxiliary stress function used is essentially that given by Jeffery [1].

### GEOMETRY OF OPENINGS

A large plate containing two circular openings as shown in Fig. 1 is best suited to the system of bipolar coordinates\* defined by the complex relation

$$z = -d \coth \frac{1}{2}i\zeta, \quad (1)$$

where  $d$  is the distance of poles on the  $x$ -axis from the origin,  $z$  and  $\zeta$  are two complex planes. With  $z = x + iy$  and  $\zeta = \xi + i\eta$ , equation (1) can be reduced to

$$\left. \begin{aligned} x &= J \sinh \eta \\ y &= J \sin \xi \end{aligned} \right\} \quad (2)$$

where

$$\frac{d}{J} = \cosh \eta - \cos \xi$$

$J$  is the stretch ratio of the coordinate transformation. Elimination of  $\xi$  from equation (2) leads to

$$(x - d \coth \eta)^2 + x^2 = d^2 \operatorname{cosech}^2 \eta. \quad (3)$$

Equation (3) clearly represents a family of coaxial circles with centers on  $(d \coth \eta, 0)$  and radii  $d \operatorname{cosech} \eta$ . Elimination of  $\eta$  from equation (2) gives rise to another family of coaxial circles which builds an orthogonal network with equation (3).

\* For a detailed discussion of bipolar coordinates, see [1].

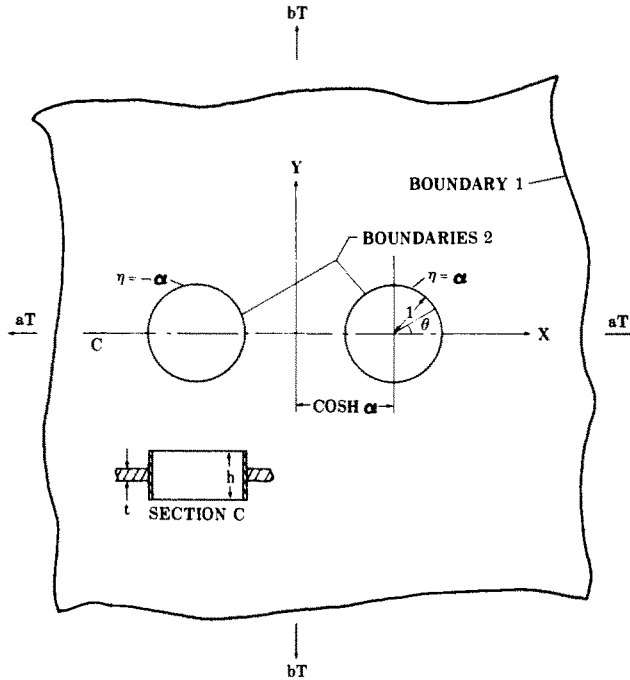


FIG. 1. Geometry of the opening.

Equation (3), with  $\eta = \pm\alpha$ , represents two symmetrical circles each of radius  $d \operatorname{cosech} \alpha$  with centers on  $(\pm d \coth \alpha, 0)$ . The ratio of the distance  $2d \coth \alpha$  between the centers of the two circles to the diameter  $2d \operatorname{cosech} \alpha$  of a circle is thus the dimensionless quantity  $\cosh \alpha$ . Figure 1 shows the relative positions of the circular openings of unit radius each.

In Fig. 1, the openings are reinforced by a circular ring of rectangular cross section. This solution, however, is related directly to the area of cross section  $A$  of the reinforcement. Therefore, the ring cross section can have any arbitrary symmetrical shape so long as its thickness is small compared to the radii of the openings. The sectional area of the material removed for the two openings is  $4t$  (since both the radii are unity), where  $t$  is the thickness of the plate. The total area of reinforcement, which we refer to as area replaced, is  $4A$ . Therefore the ratio of area replaced to area removed can be given by the dimensionless quantity,

$$\alpha' = \frac{4A}{4t} = \frac{A}{t}. \quad (4)$$

We thus have only two parametric quantities  $\cosh \alpha$  and  $\alpha'$  which respectively govern the size and separation of the symmetrical openings and the amount of reinforcing material in our theoretical model of two circular reinforced holes in a large plate.

### BOUNDARY CONDITIONS

In order for an elastic plane stress field to correspond to our specified theoretical model, the boundary stresses and strains must satisfy the following conditions:

1. At infinity, i.e., the outside boundary of the plate (Boundary 1, Fig. 1), the stresses assume given values.

2. At the junctures of the plate and the reinforcing rings (Boundaries 2, Fig. 1), the normal and shear forces in the plate equal those in the reinforcing rings.

3. At the same junctures (Boundaries 2, Fig. 1), the circumferential strains in the plate equal those in the reinforcing rings. Boundary Condition 1 follows directly from the fundamental stress state generated in the plate without openings subject to uniform stresses  $aT$  and  $bT$  (Fig. 1) at infinity.

Consideration of equilibrium of forces at Boundary 2 leads to following set of equations (see [4]):

$$\left. \begin{aligned} \frac{\partial P}{\partial s} ds + S ds &= 0 \\ R ds - P d\theta &= 0 \end{aligned} \right\} \tag{5}$$

Boundary Conditions 2 and 3 can be represented by

$$\left. \begin{aligned} R &= \widehat{\eta\eta}t \\ S &= \widehat{\xi\eta}t \end{aligned} \right\} \tag{6}$$

and

$$P = A(\widehat{\xi\xi} - \nu\widehat{\eta\eta}) \tag{7}$$

respectively, where  $\nu$  is Poisson's ratio. Equations (5), (6) and (7) can be combined to give

$$\left. \begin{aligned} \widehat{\eta\eta} &= \frac{A/t}{(ds/d\theta) + \nu(A/t)} \widehat{\xi\xi} \\ \widehat{\xi\eta} &= -\frac{\partial}{\partial s} \left[ \frac{(A/t)(ds/d\theta)\widehat{\xi\xi}}{(ds/d\theta) + \nu(A/t)} \right] \end{aligned} \right\} \tag{8}$$

In our bipolar coordinates:

$$\frac{ds}{d\theta} = \frac{d}{\sinh \eta}$$

and

$$\frac{\partial}{\partial s} = \frac{1}{J} \frac{\partial}{\partial \xi}$$

With these and equation (4), equations (8) reduce to

$$\left. \begin{aligned} \widehat{\eta\eta} &= \gamma_s \widehat{\xi\xi} \\ \widehat{\xi\eta} &= (\gamma_c - \gamma_l \cos \xi) \frac{\partial}{\partial \xi} \widehat{\xi\xi} \end{aligned} \right\} \tag{9}$$

where

$$\begin{aligned} \gamma_s &= \frac{\alpha'}{1 + \nu\alpha'} \\ \gamma_c &= \gamma_s \coth \alpha \\ \gamma_l &= \gamma_s \operatorname{cosech} \alpha. \end{aligned}$$

Equations (9) clearly reduce to the boundary conditions (Ref. [3]) for a plate containing two unreinforced holes if we let  $\alpha' = 0$ , which is of course expected.

### DETERMINATION OF STRESSES

In bipolar coordinates, the stress components are given by [1]

$$\left. \begin{aligned} d\widehat{\eta\eta} &= \left[ (\cosh \eta - \cos \xi) \frac{\partial^2}{\partial \xi^2} - \sinh \eta \frac{\partial}{\partial \eta} - \sin \xi \frac{\partial}{\partial \xi} + \cosh \eta \right] \frac{F}{J} \\ d\widehat{\xi\xi} &= \left[ (\cosh \eta - \cos \xi) \frac{\partial^2}{\partial \eta^2} - \sinh \eta \frac{\partial}{\partial \eta} - \sin \xi \frac{\partial}{\partial \xi} + \cos \xi \right] \frac{F}{J} \\ d\widehat{\xi\eta} &= -(\cosh \eta - \cos \xi) \frac{\partial^2}{\partial \eta \partial \xi} \left( \frac{F}{J} \right) \end{aligned} \right\} \quad (10)$$

where  $F$  is the Airy stress function.

The function  $F$  can be generated by superposition of a fundamental stress function  $F_0$  and an auxiliary stress function  $F_a$  such that  $F_0$  will give rise to the applied stresses at infinity whereas  $F_a$  will generate perturbation stresses only. The fundamental stress function can be given by

$$F_0 = \frac{1}{2}(ay^2 + bx^2)T \quad (11)$$

and can be transformed to

$$F_0 = \frac{J^2}{2} (a \sin^2 \xi + b \sinh^2 \eta)T \quad (12)$$

in bipolar coordinates with the aid of equations (2).

Solution of the biharmonic equation in the present notation of bipolar coordinates given by [1] is

$$\begin{aligned} \frac{F_a}{J} &= \{B_0 \eta + K \log(\cosh \eta - \cos \xi)\} (\cosh \eta - \cos \xi) \\ &+ \sum_{n=1}^{\infty} \{\phi_n(\eta) \cos n\xi + \psi_n(\eta) \sin n\xi\}. \end{aligned}$$

Because of the symmetry of the present problem, the uneven terms in the above function can be omitted and thus we have

$$\frac{F_a}{J} = K(\cosh \eta - \cos \xi) \log(\cosh \eta - \cos \xi) + \sum_{n=1}^{\infty} \phi_n(\eta) \cos n\xi \quad (13)$$

where

$$\phi_n(\eta) = A_n \cosh(n+1)\eta + B_n \cosh(n-1)\eta$$

and  $A_n$ ,  $B_n$  and  $K$  are parametric coefficients to be determined by the boundary conditions.

The coefficients can be made dimensionless by choosing the stress function  $F$  in the form\*

$$F = F_0 + dTF_a. \tag{14}$$

With the aid of equations (10), (12), (13) and (14), all the stress components can be obtained and expanded into Fourier series between  $-\pi$  and  $\pi$ ; thus

$$\left. \begin{aligned} \widehat{\eta\eta} &= \sum_0^\infty h_{1,n} \cos n\xi \\ \widehat{\xi\xi} &= \sum_0^\infty h_{2,n} \cos n\xi \\ \widehat{\xi\eta} &= \sum_1^\infty h_{3,n} \sin n\xi \end{aligned} \right\} \tag{15}$$

where  $h_{1,n}$ ,  $h_{2,n}$ , and  $h_{3,n}$  are given in the Appendix.

The first of the boundary conditions stated in the preceding section requires that the stresses assume some given values at infinity. The stress field generated by  $F$  clearly has the specified boundary values  $aT$  and  $bT$  at infinity, provided the auxiliary stresses completely vanish at infinity. This, however, requires [3] that

$$\sum_1^\infty (A_n + B_n) = 0 \tag{16}$$

Boundary conditions established by equations (9) can be satisfied by substituting equations (15) in equations (9), so that after equating to zero the coefficients of cosines of equal multiples of angles, we have

$$\left. \begin{aligned} h_{1,n} - \gamma_s h_{2,n} &= 0 \quad n \geq 0 \\ h_{3,n} - \frac{1}{2}[(n+1)h_{2,(n+1)}\gamma_l - 2nh_{2,n}\gamma_c + (n-1)h_{2,(n-1)}\gamma_l] &= 0, \quad n \geq 1 \end{aligned} \right\} \tag{17}$$

Equations (17) can be simplified and reduced to following form

$$\left. \begin{aligned} a_{n-1}A_{n-1} + b_{n-1}B_{n-1} + a_nA_n + b_nB_n + a_{n+1}A_{n+1} + b_{n+1}B_{n+1} + c_n &= 0 \quad (n \geq 0) \\ a'_{n-2}A_{n-2} + b'_{n-2}B_{n-2} + a'_{n-1}A_{n-1} + b'_{n-1}B_{n-1} + a'_nA_n + b'_nB_n + a'_{n+1}A_{n+1} \\ + b'_{n+1}B_{n+1} + a'_{n+2}A_{n+2} + b'_{n+2}B_{n+2} + c'_n &= 0 \quad (n \geq 1) \end{aligned} \right\} \tag{18}$$

where  $a_{n-1}$ ,  $b_{n-1}$ ,  $a_n$ ,  $b_n$ ,  $a_{n+1}$ ,  $b_{n+1}$ ,  $c_n$ ,  $a'_{n-2}$ ,  $b'_{n-2}$ ,  $a'_{n-1}$ ,  $b'_{n-1}$ ,  $a'_n$ ,  $b'_n$ ,  $a'_{n+1}$ ,  $b'_{n+1}$ ,  $a'_{n+2}$ ,  $b'_{n+2}$  and  $c'_n$  are constants depending on the geometry of the problem and are included in the Appendix.

Equations (16) and (18) represent the solution of the problem. Theoretically, all the required coefficients  $A_n$ ,  $B_n$ , and  $K$  can be calculated from the above set of infinite equations; however, this is quite intricate. Thus it is desirable to limit the value of  $n$  and consider the finite system of equations on the assumption that the coefficients  $A_n$  and  $B_n$  converge. With  $n = r$ , we obtain  $2r + 5$  coefficients (including  $K$ ) to be determined from  $2r + 2$  equations, as can be seen from equations (16) and (18) and the Appendix. This inconsistency in the set of equations can be easily removed if we recall equations (15). On the basis of assumed

\* This stress function was used in [3] for determining stresses around two unreinforced circular holes in a plate subject to plane stresses.

convergence and  $n = r$ , equations (15) suggest that

$$\left. \begin{aligned} h_{1,(n+1)} &= 0 \\ h_{2,(n+1)} &= 0 \\ h_{3,(n+1)} &= 0 \end{aligned} \right\}. \quad (19)$$

Thus the system of equations (16) and (18) together with equations (19) is now capable of determining all the coefficients  $A_n$ ,  $B_n$ , and  $K$ . These coefficients can then be substituted in the expressions for  $h_{1,n}$ ,  $h_{2,n}$ , and  $h_{3,n}$  (see Appendix) used to compute the individual stresses from equations (15) as functions of the variable  $\xi$ .

Lastly, for convenience, we shall define the polar angle  $\theta$ , as shown in Fig. 1, in terms of bipolar coordinates by

$$\cos \xi = \frac{1 + \cosh \eta \cos \theta}{\cosh \eta + \cos \theta}. \quad (20)$$

For any particular set of two circles given by  $\eta = \pm \alpha$ ,  $\cos \xi$  can now easily be computed for any point on the circles defined by  $\theta$ .

## NUMERICAL RESULTS

The method outlined in previous sections for computing stresses in a plate containing two equal reinforced circular holes was programmed for a digital computer. Stress concentration factors, defined as the ratio of the maximum tangential stress in the plate at the opening to the applied stress, were calculated at intervals of 10 degrees around the opening for all combinations of the following values of the parameters  $\cosh \alpha$  and  $\alpha'$ :

$$\cosh \alpha = 1.2, 1.3, 1.4, 1.5, 1.75, 2.0, 2.5, 3 \text{ and } 4$$

$$\alpha' = 0, 0.02, 0.05, 0.10, 0.15, 0.20, 0.30, 0.40, 0.50, 0.60, 0.80, 1.0, 1.5, 2.0 \text{ and } 10^8.$$

Two load cases of  $aT = 0$ ,  $bT = 1$  (transverse tension) and  $aT = 1$ ,  $bT = 0$  (longitudinal tension) were considered. With the aid of these two load cases, any desired state of biaxial stress could be generated by linearly superimposing suitable fractions or multiples of individual applied stresses. Values of stress concentration factors for the above cases with  $aT = 0$ ,  $bT = 1$  and  $aT = 1$ ,  $bT = 0$  as functions of  $\theta$  (the polar angle) were computed and only typical cases have been reported in the various tables and diagrams in this paper.

The closest spacing of the two openings for which the computer program would give acceptable convergence was  $\cosh \alpha = 1.2$ . Values larger than  $\cosh \alpha = 4$  gave rise to very large numbers which exceeded the capacity of the computing facility within the coded program. Although smaller values of  $\cosh \alpha$  and  $\alpha'$  were the main objective of the investigation, larger values ( $\cosh \alpha > 2$  and  $\alpha' > 1.0$ ) were also included to demonstrate the validity of the solution (see next section).

The value of  $n$ , where the system converged, was varied from 15 to 23 depending on  $\cosh \alpha$ . Therefore the maximum number of equations solved was  $2n + 5$  which, for  $n = 23$ , was 51.

Poisson's ratio was assumed to be 0.3 for these calculations.

Stress concentration factors based on the maximum strain energy of distortion were also computed for a few cases; see Fig. 4. These stress concentration factors serve as a good guide in considering structural failures.

## DISCUSSION OF RESULTS

In the present investigation, the stress concentration factors are also, by definition, the actual stresses since the applied stress is always taken as unity. Hereafter only the term stresses will be used. Tables 1 and 2 include the stresses  $\xi\xi$  for  $\alpha' = 0$ , i.e., no reinforcement. These stresses are the same as determined by Ling [3], who, in contrast to the present paper, computed these stresses in closed form.

TABLE 1. TANGENTIAL STRESS AT  $\theta = 180^\circ$  VS COSH  $\alpha$  FOR VARIOUS AMOUNTS OF REINFORCEMENTS; TRANSVERSE LOAD ( $aT = 0, bT = 1$ )

$\alpha'$ \ Cosh $\alpha$	1.2	1.3	1.4	1.5	1.75	2.0	2.5	3.0	4.0
0%	4.423	3.768	3.442	3.264	3.077	3.020	2.994	2.992	2.995
5%	3.672	3.258	3.040	2.916	2.777	2.729	2.703	2.697	2.695
20%	2.562	2.399	2.305	2.248	2.178	2.151	2.132	2.125	2.122
40%	1.911	1.842	1.799	1.772	1.738	1.723	1.712	1.708	1.703
100%	1.202	1.193	1.186	1.182	1.177	1.174	1.172	1.172	1.171
108%	0.377	0.386	0.392	0.397	0.403	0.406	0.409	0.410	0.412

TABLE 2. TANGENTIAL STRESS AT  $\theta = 90^\circ$  VS. COSH  $\alpha$  FOR VARIOUS AMOUNTS OF REINFORCEMENTS; LONGITUDINAL LOAD ( $aT = 1, bT = 0$ )

$\alpha'$ \ Cosh $\alpha$	1.2	1.3	1.4	1.5	1.75	2.0	2.5	3.0	4.0
0%	2.580	2.593	2.608	2.623	2.663	2.703	2.772	2.825	2.891
5%	2.320	2.334	2.349	2.364	2.403	2.440	2.504	2.550	2.605
20%	1.843	1.856	1.869	1.882	1.915	1.944	1.991	2.023	2.060
40%	1.503	1.513	1.524	1.535	1.560	1.582	1.616	1.638	1.663
100%	1.058	1.065	1.072	1.078	1.094	1.107	1.125	1.137	1.151
108%	0.389	0.391	0.392	0.394	0.398	0.400	0.403	0.407	0.409

Figures 2 and 3 summarize the influence of reinforcement. As in the case of a single opening, reinforcement seems to be most effective in the beginning. The maximum stress comes down asymptotically to a limit when  $\alpha' = \infty$  (rigid reinforcement). In this investigation at  $\alpha' = 10^8$  (practically rigid), the maximum stress was found to be 0.377 at  $\cosh \alpha = 1.2$  and 0.412 at  $\cosh \alpha = 4$ ; these values agree well with those given in Ref. [4] for a single reinforced circular hole. The most effective amount of reinforcement seems to be approximately 40% because any further reduction in stress would be at the cost of larger increases in the amount of reinforcement.



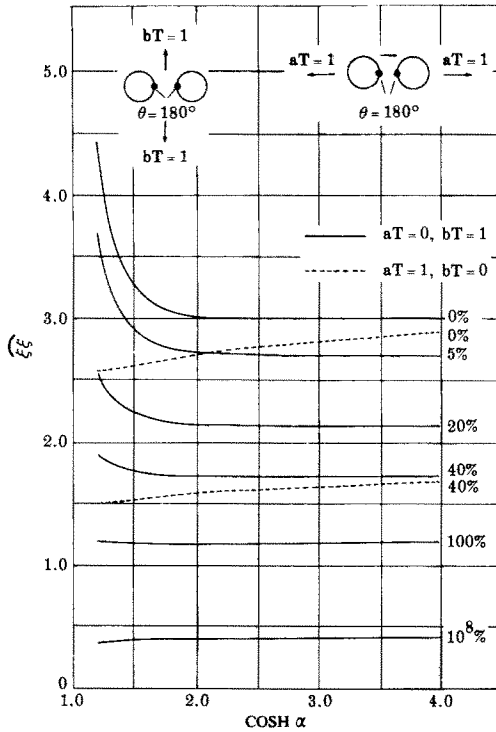


FIG. 2. Maximum tangential stress vs.  $\cosh \alpha$  for various amounts of reinforcements.

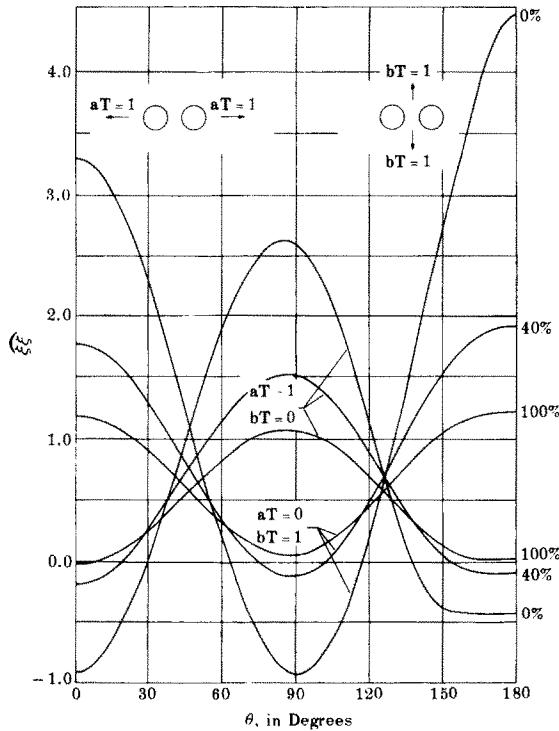


FIG. 3. Tangential stress vs.  $\theta$  for 0%, 40% and 100% reinforcement and  $\cosh \alpha = 1.2$ .

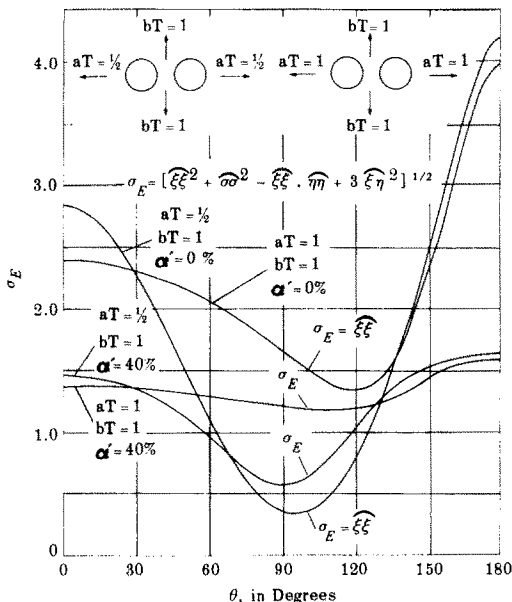


FIG. 4. Maximum equivalent stresses  $\sigma_E$  vs.  $\theta$  for 0% and 40% reinforcements.

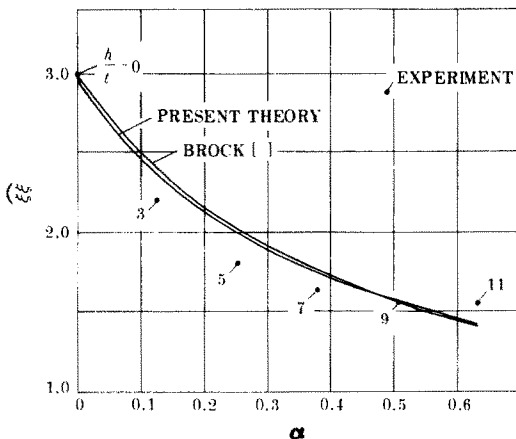


FIG. 5. Comparison of maximum tangential stress for  $\cosh \alpha = 4$  with other theory and experiment.

Figure 2 indicates that  $\cosh \alpha = 2$ , the two openings behave almost like a single opening since for practical purposes, all the curves in the transverse tension case become asymptotic from this point onwards. The maximum deviation from the asymptotic value is 1.25% for  $\alpha' = 0.05$ .

Figure 4 shows the equivalent stress  $\sigma_E$  based on the maximum strain energy of distortion theory. These stresses are listed for  $\cosh \alpha = 1.2$  and  $\alpha' = 0$  and 0.4. The load cases are similar to those found in spherical or cylindrical pressure vessels. The highest stress with  $\alpha' = 0$  when  $aT = \frac{1}{2}$  and  $bT = 1$  drops down to 1.632 from 4.209 when  $\alpha' = 0.4$ .

A parabolic interpolation in the neighborhood of the largest stress in the longitudinal tension case, (i.e.,  $aT = 1, bT = 0$  with  $\cosh \alpha = 1.2$  and  $\alpha' = 0$ ) determined that the

actual maximum stress occurred at  $\theta \simeq 84.6^\circ$ . The magnitude of this actual maximum stress was 2.618 rather than 2.591 as shown in Fig. 3 at  $\theta = 80^\circ$ . In general, this maximum stress occurred in the vicinity of  $\theta = 90^\circ$  and the actual shift was towards  $\theta = 0^\circ$ . The magnitude of this shift depends on the closeness of the other opening and the amount of reinforcement. For practical purposes, however, the maximum stress can be assumed to occur at  $\theta = 90^\circ$ .

Figure 5 compares the results of Brock [6] for a single reinforced circular opening with the present theory when  $\cosh \alpha = 4$ . In the theory of Ref. [6] the reinforcing ring, in contrast to present theory, has discrete dimensions which define the distribution of the area of reinforcement. The factor  $h/t$  is the ratio of the height of the rectangular reinforcing ring to the plate thickness  $t$  (Fig. 1). The results of [6] plotted in Fig. 5 are in fact the stresses at the inside boundary of the ring whereas the present theory assumes the ring to be so thin that the maximum stress in the plate should be a good approximation for the maximum stress in the reinforcing ring. The two curves show a remarkable degree of agreement. The experimental results of [7] are also in reasonable agreement with both the theories; the largest deviation is 10% at  $\alpha' = 0.25$ .

## CONCLUSIONS

The interaction between the two openings is not very significant when  $\cosh \alpha \geq 2$ , i.e., when the distance between the inner edges of the two circular openings is one diameter or greater. For  $\cosh \alpha > 2$ , this influence is relatively more pronounced in the longitudinal case than in the transverse tension case.

The most effective amount of reinforcement appears to be near 40% area replacement, whereas any additional amount of reinforcement does not produce a proportionate reduction of the stresses. With the above amount of reinforcement, the two openings can be as close as  $\cosh \alpha = 1.2$ , i.e., the distance between their inner edges is 20% of the diameter; the effective stress comes down from 4.209 to 1.632.

For the limiting case of a single opening and the assumption of compact reinforcement, the present theory agrees with other available experiments and theories up to  $\alpha' = 0.6$ .

*Acknowledgements*—The author wishes to express his sincere appreciation to the Naval Ship Engineering Center for sponsoring the research embodied in this paper. The author also wishes to thank Mr. J. S. Brock for his fruitful comments throughout this investigation and Mr. J. Ogelsby who successfully coded this solution for execution on a digital computer.

## REFERENCES

- [1] G. B. JEFFERY, Plane stress and plane strain in bipolar coordinates. *Phil. Trans. R. Soc.* **A221**, 265–293 (1921).
- [2] R. D. MINDLIN, Stress distribution around a hole near the edge of a plate under tension. *Proc. Soc. exp. Stress Analysis* **5**, 56–68 (1948).
- [3] C. B. LING, On the stresses in a plate containing two circular holes. *J. appl. Phys.* **19**, 77–82 (1948).
- [4] J. R. M. RADOK, Problems of plane elasticity for reinforced boundaries. *J. appl. Mech. Trans. ASME* **77**, 249–254 (1955).
- [5] H. REISSNER and M. MORDUCHOW, Reinforced circular cutouts in plane sheets. *NACA TN 1852* (April 1949).
- [6] J. S. BROCK, The stresses around reinforced circular and square holes with rounded corners in a plate subjected to tensile load. *Naval Ship Res. Dev. Center Rep.* In preparation.
- [7] C. M. KUNTSMANN and R. C. UMBERGER, The stresses around reinforced square openings with rounded corners in a uniformly loaded plate. Thesis, Webb Institute of Naval Architecture (June 1959).

## APPENDIX

Coefficients of equations (15):

$$\begin{aligned}
 h_{1,n} = & L_n - \frac{K}{2} \{ \delta_{0,n} \cosh 2\eta - 2\delta_{1,n} \cosh \eta + \delta_{2,n} \} \\
 & + \frac{1}{2} \{ (n-1)(n-2) [A_{n-1} \cosh n\eta + B_{n-1} \cosh(n-2)\eta] \\
 & - 2(n^2-1) [A_n \cosh(n+1)\eta + B_n \cosh(n-1)\eta] \cosh \eta \\
 & + (n+1)(n+2) [A_{n+1} \cosh(n+2)\eta + B_{n+1} \cosh n\eta] \\
 & - 2[(n+1)A_n \sinh(n+1)\eta + (n-1)B_n \sinh(n-1)\eta] \sinh \eta \}, \quad n \geq 0
 \end{aligned}$$

where  $\delta_{m,n}$  is Kronecker delta.

$$\begin{aligned}
 h_{2,n} = & M_n + \frac{K}{2} \{ \delta_{0,n} \cosh 2\eta - 2\delta_{1,n} \cosh \eta + \delta_{2,n} \} \\
 & - \frac{1}{2} \{ [n^2 A_{n-1} \cosh n\eta + (n-2)^2 B_{n-1} \cosh(n-2)\eta] \\
 & - 2[(n+1)^2 A_n \cosh(n+1)\eta + (n-1)^2 B_n \cosh(n-1)\eta] \cosh \eta \\
 & + [(n+2)^2 A_{n-1} \cosh(n+2)\eta + n^2 B_{n+1} \cosh n\eta] \\
 & + (n-2) [A_{n-1} \cosh n\eta + B_{n-1} \cosh(n-2)\eta] \\
 & + 2[(n+1)A_n \sinh(n+1)\eta + (n-1)B_n \sinh(n-1)\eta] \sinh \eta \\
 & - (n+2) [A_{n+1} \cosh(n+2)\eta + B_{n+1} \cosh n\eta] \}, \quad n \geq 0 \\
 h_{3,n} = & N_n - \delta_{1,n} K \sinh \eta \\
 & - \frac{1}{2} \{ (n-1) [n A_{n-1} \sinh n\eta + (n-2) B_{n-1} \sinh(n-2)\eta] \\
 & - 2n [A_n (n+1) \sinh(n+1)\eta + B_n (n-1) \sinh(n-1)\eta] \cosh \eta \\
 & + (n+1) [(n+2) A_{n+1} \sinh(n+2)\eta + n B_{n+1} \sinh n\eta] \}, \quad n \geq 1.
 \end{aligned}$$

Coefficients of equations (18):

$$\begin{aligned}
 a_{n-1} &= \left[ \frac{(n-1)(n-2)}{2} + \frac{\gamma_s n^2}{2} + \frac{\gamma_s (n-2)}{2} \right] \cosh n\eta \\
 b_{n-1} &= \left[ \frac{(n-1)(n-2)}{2} + \frac{\gamma_s (n-2)^2}{2} + \frac{\gamma_s (n-2)}{2} \right] \cosh(n-2)\eta \\
 a_n &= -[(n^2-1) + \gamma_s (n+1)^2] \cosh(n+1)\eta \cosh \eta - (n+1)(1-\gamma_s) \sinh(n+1)\eta \sinh \eta \\
 b_n &= -[(n^2-1) + \gamma_s (n-1)^2] \cosh(n-1)\eta \cosh \eta - (n-1)(1-\gamma_s) \sinh(n-1)\eta \sinh \eta \\
 a_{n+1} &= \left[ \frac{(n+1)(n+2)}{2} + \frac{\gamma_s (n+2)^2}{2} - \frac{\gamma_s (n+2)}{2} \right] \cosh(n+2)\eta
 \end{aligned}$$

$$b_{n+1} = \left[ \frac{(n+1)(n+2)}{2} + \frac{\gamma_s n^2}{2} - \frac{\gamma_s(n+2)}{2} \right] \cosh n\eta$$

$$c_n = [L_n - \gamma_s M_n] - (1 + \gamma_s) \frac{K}{2} [\delta_{0,n} \cosh 2\eta - 2\delta_{1,n} \cosh \eta + \delta_{2,n}].$$

Above equations are valid only for  $\eta = \pm\alpha$  and for  $n \geq 0$ .

Following equations are valid only at  $\eta = \pm\alpha$  and  $n \geq 1$ .

$$a'_{n-2} = -[(n-1)^2 + (n-3)] \frac{(n-1)}{4} \gamma_l \cosh(n-1)\eta$$

$$b'_{n-2} = -[(n-3)^2 + (n-3)] \frac{(n-1)}{4} \gamma_l \cosh(n-3)\eta$$

$$a'_{n-1} = -\frac{1}{2} \{ [\sinh n\eta \sinh \eta - n \cosh n\eta \cosh \eta] n(n-1) \gamma_l \\ - [n^2 + (n-2)] n \gamma_c \cosh n\eta - n(n-1) \sinh n\eta \}$$

$$b'_{n-1} = -\frac{1}{2} \{ [\sinh(n-2)\eta \sinh \eta - (n-2) \cosh(n-2)\eta \cosh \eta] (n-1)(n-2) \gamma_l \\ - [(n-2)^2 + (n-2)] n \gamma_c \cosh(n-2)\eta - (n-1)(n-2) \sinh(n-2)\eta \}$$

$$a'_n = -\frac{1}{2} \left\{ \frac{n(n^2-1)}{2} \gamma_l \cosh(n+1)\eta + 2[(n+1) \cosh(n+1)\eta \cosh \eta \right. \\ \left. - \sinh(n+1)\eta \sinh \eta] n(n+1) \gamma_c + [(n+1)^2 + (n-1)] \cosh(n+1)\eta \frac{(n+1) \gamma_l}{2} \right. \\ \left. + 2n(n+1) \sinh(n+1)\eta \cosh \eta \right\}$$

$$b'_n = -\frac{1}{2} \left\{ [(n-1)^2 - (n+1)] \frac{(n-1)}{2} \gamma_l \cosh(n-1)\eta \right. \\ \left. + 2[(n-1) \cosh(n-1)\eta \cosh \eta - \sinh(n-1)\eta \sinh \eta] n(n-1) \gamma_c \right. \\ \left. + \frac{n(n^2-1)}{2} \gamma_l \cosh(n-1)\eta + 2n(n-1) \sinh(n-1)\eta \cosh \eta \right\}$$

$$a'_{n+1} = -\frac{1}{2} \{ -n(n+1)(n+2) \gamma_c \cosh(n+2)\eta - [(n+2) \cosh(n+2)\eta \cosh \eta \\ - \sinh(n+2)\eta \sinh \eta] (n+1)(n+2) \gamma_l - (n+1)(n+2) \sinh(n+2)\eta \}$$

$$b'_{n+1} = -\frac{1}{2} \{ -[n^2 - (n+2)] n \gamma_c \cosh n\eta - [n \cosh n\eta \cosh \eta \\ - \sinh n\eta \sinh \eta] n(n+1) \gamma_l - n(n+1) \sinh n\eta \}$$

$$a'_{n+2} = -\frac{(n+1)(n+2)(n+3)}{4} \gamma_l \cosh(n+3)\eta$$

$$b'_{n+2} = -\frac{(n+1) \gamma_l}{4} [(n+1)^2 - (n+3)] \cosh(n+1)\eta$$

$$c'_n = \frac{(n+1) \gamma_l}{2} M_{n+1} - n \gamma_c M_n + \frac{(n-1) \gamma_l}{2} M_{n-1} - N_n + \frac{(n+1) \gamma_l}{2} K_{2,(n+1)}$$

$$-n\gamma_c K_{2,n} + \frac{(n-1)\gamma_l}{2} K_{2,(n-1)} - K_{3,n}$$

where,

$$K_{2,n} = -K[\delta_{1,n} \cosh \eta - \frac{1}{2}\delta_{2,n}]$$

$$K_{3,n} = -K\delta_{1,n} \sinh \eta$$

$$L_0 = e^{-\eta}(a \cosh \eta + b \sinh \eta)$$

$$M_0 = e^{-\eta}(a \sinh \eta + b \cosh \eta)$$

$$L_n = -M_n = N_n = 2(a-b)e^{-n\eta} \sinh \eta (n \sinh \eta - \cosh \eta), \quad n \geq 1.$$

(Received 15 January 1968; revised 15 March 1968)

**Абстракт**—Дается аналитическое решение для напряжений вокруг двух круглых отверстий равного размера в тонкой упругой пластинке, из изотропного материала, под влиянием двухосной нагрузки. Отверстия могут быть неусиленные или усиленные. Усиливающий материал, являющийся, таким же самым как материал исходной пластинки, окружает края отверстий. Получаются напряжения в виде бесконечных рядов, используя биполярные координаты. Численная сходимость этих рядов обеспечена отношением размера и расстояния двух отверстий. Результаты вычислены на электронной счетной машине и представлены в форме концентрации напряжений для некоторого числа геометрий отверстий и усилений, которые случаются на практике.